# Analysis of variable-order interacting multiple model algorithms for cell tracking



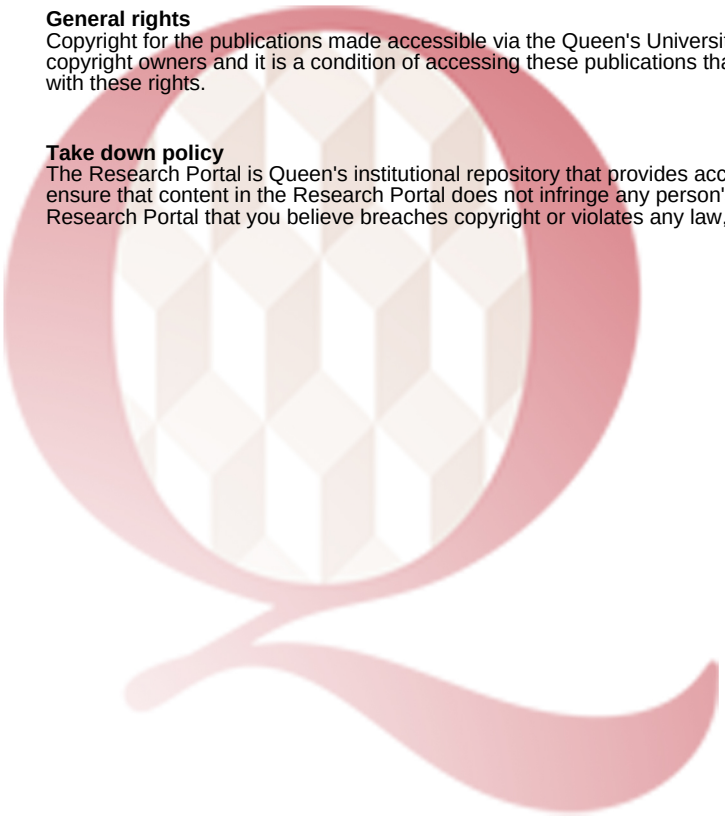

# Analysis of variable-order interacting multiple model algorithms for cell tracking

x

*x*

**Abstract**

In this paper we propose a modification of the Interacting Multiple Model (IMM) filter to effectively track complex dynamics in cell images. Our solution proposes a more efficient use and combination of the multiple Kalman filter estimations that lead to a performance improvement in multi-cell sequences, with an increase of up to 10% in the recall value, compared to the classic IMM. First and second order models are evaluated in the scope of cell migration. The system is evaluated and compared against a baseline using 3D synthetic confocal microscopy images, where cells behave realistically according to actual cell trajectories extracted from real sequences in biology.

**Keywords:** Live Cell Tracking, Particle Tracking, IMM Filter, Second-Order Markov Chains

## 1 Introduction

Progress in medicine significantly depends on developing a deeper understanding of cell movements and cell interactions. Recent developments in stochastic and deterministic super-resolution microscopy techniques yield images with a resolution below the diffraction limit [Huang et al., 2009], giving biologists the technology to observe processes at the nanometre scale in real time, which was not possible before. In spite of all the advantages that new technologies have brought, some challenges associated with them have also arisen, such as the large amount of raw data which needs to be processed to extract precise information, obtain quantitative characterizations of the observed phenomena, and draw meaningful conclusions [Meijering et al., 2006]. Thus, automated acquisition and analysis of cell images has become more and more essential for biomedical research over the past 15 years [Peng, 2008].

Among the features that can be extracted and analysed automatically, the migration and mobility of a cell in a 3D environment is crucial for understanding an immune response and wound healing [Pivarcsi et al., 2004, Gurtner et al., 2008]. Automatic tracking of moving cells can also be used to perform the required continuous adjustments needed to keep the objects of interest within the imaging field and in focus. However, multiple cell tracking is a complex task that is far from being solved, given the variety of behaviours and interactions that cells can express in different sequences, including migration, crawling, splitting, and phagocytosis, to name a few. This diversity requires the use of one or multiple complex motion models that must be selected and combined to ensure an accurate and robust tracking.

In this paper, we investigate the use of tracking algorithms to extract trajectories from multiple cells moving in a 3D environment. In particular, the use of the Interacting Multiple Model (IMM) filter is proposed given its ability to combine different motion models at every given time. A novel approach to the combination of multiple model estimations is proposed, which surpasses the traditional approach.

Given the limited amount of real data obtained via confocal microscopy, the system is evaluated using realistic 3D synthetic images. The trajectories of the moving objects correspond to cell trajectories extracted from real sequences in biology [de Solórzano et al., 2015] to ensure natural behaviours and interactions [Wilson et al., 2016].

## 2 State of the Art

Traditionally, cell detection, segmentation, and tracking used to be performed manually (by pointing and clicking the objects of interest on each frame). However, several reasons make such a task tedious, or even impossible. First, the datasets are now so large [Meijering et al., 2006, Peng, 2008], that manually processing them would take days, and selecting smaller subsets means losing relevant information and taking biased decisions. Second, manually determining the centroids of the cells is a user-dependent measurement, and as such is particularly error prone. Over the last years, a large research effort in computer science has been directed at developing effective automatic tracking algorithms.

Until recently, deterministic approaches were mostly used for cell tracking [Meijering et al., 2006]. These approaches consist of detecting the cells on each frame, and then linking them to form tracks through data association. As a consequence, these methods highly depend on the performance of the segmentation algorithm. While tracking by detection works effectively in other related fields, such as video surveillance, it struggles in biological applications due to the diverse and generally poor quality of biomedical and cell images and their low signal to noise ratio. These approaches are also impacted by the lack of specific and reliable cell detectors, therefore relying on general purpose segmentation such as simple thresholding or slightly more complex methods such as the watershed transform [Meijering et al., 2006] or wavelet transform [Genovesio et al., 2006].

As an alternative, a significant number of algorithms using a probabilistic approach, known as Bayesian tracking, have been proposed. The basic principle is to infer the current state using the observation and the previous states. These probabilistic approaches show better results [Jaqaman et al., 2008], especially when frequent segmentation errors are expected. The Kalman filter [Kalman, 1960] is a common approach, which is optimal in the case of Gaussian distributions. However, this assumption is not correct in cell motion, in particular for multi-target problems. The particle filter [Doucet and Johansen, 2011], which is based on the same principle, deals with non Gaussian and non linear cases, that are biologically relevant. However, it suffers from high complexity and particle degeneration that also imply the use of specific assumptions. As an intermediate solution, the IMM algorithm was presented in [Genovesio et al., 2006] as a novel method for tracking multiple microscopic objects in 3D space, in real-time. This solution combines several Kalman filters with different dynamic models to quickly adapt to changes of state. It is nonetheless difficult to choose relevant models for biological processes as well as determining the optimal combination of those models to deal with complex dynamics in multi-target interacting scenarios.

## 3 Interacting Multiple Model filter

The IMM filter is a Bayesian iterative algorithm that uses a combination of several Kalman filters, which allow estimating the state of a tracked object $X_k$ at a given time $k$ as a combination of several dynamical models' estimations.

Assuming $N$ dynamic models are being considered to model the most frequent behaviours of the tracked objects, each corresponding dynamic model can be expressed as a transition matrix $D^i$ for $i \in [\![1, N]\!]$, following conventional notation. Thus, given the estimated state $\hat{X}_k$ and uncertainty $\hat{C}_k$ for each tracked object at the previous time step, $N$ predictions for the new time step $k+1$, as well as their corresponding uncertainties $C^i$, are calculated using the equations:

$$X^i_{\text{pred},k+1} = D^i \tilde{X}^i_k \tag{1}$$

$$C^i_{\text{pred},k+1} = D^i \tilde{C}^i_k {D^i}^T + Q_i \tag{2}$$

where $Q_i$ is the process noise covariance, and $\tilde{X}^i_k$ and $\tilde{C}^i_k$ are the mixed state and covariance, such that:

$$\tilde{X}^i_k = \sum_{j=1}^{N} u_k^{j|i} \hat{X}^j_k \tag{3}$$

$$\tilde{C}_k^i = \sum_{j=1}^{N} u_k^{j|i} \left[ \hat{C}_k^j + \left( \hat{X}_k^j - \tilde{X}_k^j \right) \left( \hat{X}_k^j - \tilde{X}_k^j \right)^T \right] \tag{4}$$

where $u_k^{j|i} = \dfrac{1}{u_{\text{pred},k+1}^i} p_{ji} u_k^j$ is the conditional model probability, with $u_{\text{pred},k+1}^i = \sum_{j=1}^{N} p_{ji} u_k^j$ the predicted model probability, and $p_{ji}$ the probability to switch from the $j^{\text{th}}$ to the $i^{\text{th}}$ model between $k$ and $k+1$.

Each of these predictions should be compared at present time $k+1$ against the observation $Z_{k+1}$ provided by the segmentation algorithm to validate the adequacy of the chosen motion model to the current target motion.

$$\hat{X}_{k+1}^i = X_{\text{pred},k+1}^i + G_{k+1}^i \left( Z_{k+1} - H X_{\text{pred},k+1}^i \right) \tag{5}$$

$$\hat{C}_{k+1}^i = C_{\text{pred},k+1}^i \left( I - G_{k+1}^i H \right) \tag{6}$$

$I$ being the identity matrix, $H$ the observation matrix and $G$ the Kalman gain such that

$$G_{k+1}^i = C_{\text{pred},k+1}^i H^T \left( H C_{\text{pred},k+1}^i H^T + R \right)^{-1} \tag{7}$$

where $R$ is the measurement noise covariance.

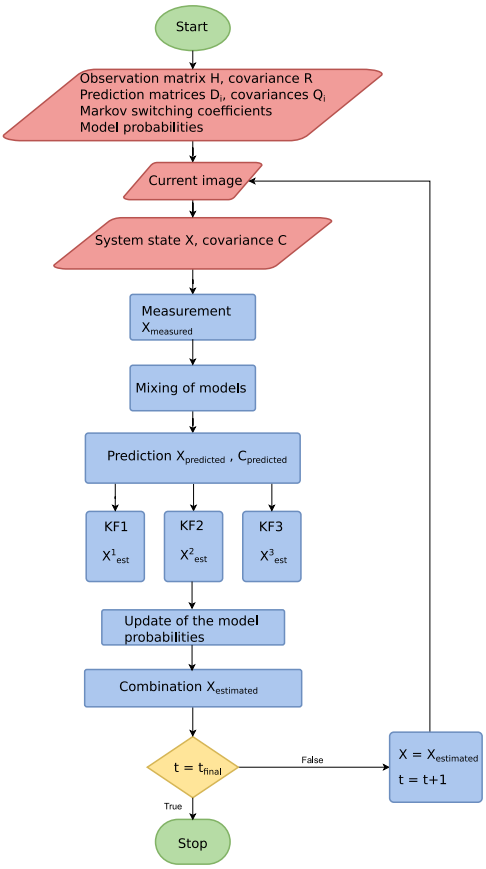

Figure 1: The IMM algorithm.

Since none of the used models is likely to provide a perfect match and the behaviour of the tracked object can be better explained as a combination of them all, the IMM computes the final combined estimated state and covariance as a weighted average of the individual estimates:

$$\hat{X}_{k+1} = \sum_{i=1}^{N} u_{k+1}^i \hat{X}_{k+1}^i \tag{8}$$

$$\hat{C}_{k+1} = \sum_{i=1}^{N} u_{k+1}^i \left[ \hat{C}_{k+1}^i + \left( \hat{X}_{k+1}^i - \hat{X}_{k+1} \right) \left( \hat{X}_{k+1}^i - \hat{X}_{k+1} \right)^T \right] \tag{9}$$

A flow diagram of the algorithm is shown in Figure 1.

### 3.1 Model probabilities

The weights $u_{k+1}^i$ used in equations 8 and 9 are normalised factors proportional to the likelihood $\ell_k^i$ of how well each dynamic model $i$ fits the observation at each time instant $k$:

$$u_{k+1}^i = \frac{1}{\sum_{j=1}^{N} u_{\text{pred},k+1}^j \ell_{k+1}^j} u_{\text{pred},k+1}^i \ell_{k+1}^i \tag{10}$$

where $\ell_{k+1}^i$ is the likelihood of the filter $i$ matched to the model $i$ and is computed as follows:

$$\ell_{k+1}^{i} = \frac{1}{\sqrt{\det\left(2\pi S_{k+1}^{i}\right)}} \exp\left[-\frac{1}{2}\left(Z_{k+1} - HX_{\text{pred},k+1}^{i}\right)^{T}\left(S_{k+1}^{i}\right)^{-1}\left(Z_{k+1} - HX_{\text{pred},k+1}^{i}\right)\right] \tag{11}$$

with $S_{k+1}^{i}$ defined as the covariance of the innovation of the $i$-th Kalman filter.

The use of these model probabilities allows the IMM to effectively track an object if its movement approximately matched any of the dynamic models or combination of them. Since these weights are recalculated at each time step $k$, the behaviour of the tracked object can vary over time from one dynamic model or behaviour to another while still being effectively tracked by the IMM.

### 3.2 Second-order Markov chain based IMM

While the weighting process described in the previous section is effective, non-accurate estimations may happen due to noisy observations and wrong model choices. In order to filter some of those errors, in this section we employ an improved calculation of the model probabilities based on the assumption that the current model combination depends on the two previous time steps. This process is coherent with cell migration, whose motion and behaviour tend to be consistent over short periods of time, once the chosen cell mechanism has been initiated.

An efficient way to integrate second-order information was designed in [Lan et al., 2013] for manoeuvring target tracking applications. We applied this method, called SIMM (Second-order Markov chain based IMM) algorithm, to biological data for the first time. The difference with the classic IMM, based on a first order Markov chain, is that before the interaction step given by the equations 3 and 4, there is an additional step that consists of updating the switching probabilities $p_{ij}^{k}$, following the equations below:

$$p_{ij}^{k} = \sum_{l=1}^{N} p_{l,j,i} \times \mu_{i,l}^{k} \tag{12}$$

where $p_{l,j,i}$ are the transition probabilities of the second-order Markov chains and

$$\mu_{i,l}^{k} = \frac{1}{\sum_{q=1}^{N} u_{k-1}^{q|i}\,\ell_{k}^{i|q}}\, u_{k-1}^{l|i}\,\ell_{k}^{i|l} \tag{13}$$

where $\ell_{k}^{i|l}$ is the past likelihood of the filter $l$ matched to the model $i$:

$$\ell_{k}^{i|l} = \frac{1}{\sqrt{\det\left(2\pi S_{k}^{i|l}\right)}} \exp\left[-\frac{1}{2}\left(Z_{k} - HD^{i}\widehat{X}_{k-1}^{l}\right)^{T}\left(S_{k}^{i|l}\right)^{-1}\left(Z_{k} - HD^{i}\widehat{X}_{k-1}^{l}\right)\right] \tag{14}$$

with $S_{k}^{i|l}$ defined as the covariance of the innovation of the $i$-th Kalman filter using the estimation from the $l$-th Kalman filter.

### 3.3 Hard estimation of combined state

Finally we propose a novel modification to both the IMM and SIMM. While previous approaches estimate the best possible combination of model at each time step, this estimated state $\hat{X}_k$ and covariance $\hat{C}_k$ are not directly used in the next prediction but replaced by the mixed state and covariance $\tilde{X}_k$ and $\tilde{C}_k$. We hypothesize that since this mixed variable relies on $p_{ij}$ and $p_{l,i,j}$, which are manually or empirically chosen and fixed for every sequence, this decision may not provide a better reference for each individual predictions than the agreed previous estimation. Therefore, in our modified versions, we replace equations 1 and 2 by:

$$X_{\text{pred},k+1}^{i} = D^{i}\widehat{X}_{k} \tag{15}$$

$$C^i_{\text{pred},k+1} = D^i \widehat{C}_k {D^i}^T + Q_i \tag{16}$$

We will refer to these algorithms as the modified IMM and modified SIMM.

### 3.4 Data association

Since our application aims to track multiple objects, data association between each of the $M$ tracked objects $\{\widehat{X}_{k+1}\}_m$ for $m \in [\![1, M]\!]$ and the observations $\{Z_{k+1}\}_m$ must be solved to ensure a correct allocation of observation and predictions and a correct object tracking without identity swapping.

Following a common strategy in biology [Genovesio et al., 2006], we make use of a greedy linear assignment association in this paper.

## 4 Experiments

### 4.1 Filter setup

In order to track cells in 3D confocal microscopy, the (x, y, z) positions of their centroids must be included as variables in the state vector. Given the need of modelling first and second order motion models to explain cell migration, velocity and acceleration vectors are also coded, resulting in the state vector:

$$X_k = (x_k, y_k, z_k, x_{k-1}, y_{k-1}, z_{k-1}, x_{k-2}, y_{k-2}, z_{k-2})^T$$

Three different dynamical models are chosen for our IMM implementation: constant velocity (CV), constant acceleration (CA) and Brownian motion (BM). All three models are common behaviours for biological objects [Genovesio et al., 2006], such as cells or even smaller particles (organelles, viruses, etc.). We represent the CV model by a linear extrapolation of the locations, the CA by a linear extrapolation of the velocities, and the BM by adding Gaussian noise to the previous state. They are coded as the following transition matrices:

$$D_{\text{CV}} = \begin{pmatrix} 2 & 0 & 0 & -1 & 0 & 0 & 0 & 0 & 0 \\ 0 & 2 & 0 & 0 & -1 & 0 & 0 & 0 & 0 \\ 0 & 0 & 2 & 0 & 0 & -1 & 0 & 0 & 0 \\ 1 & 0 & 0 & 0 & 0 & 0 & 0 & 0 & 0 \\ 0 & 1 & 0 & 0 & 0 & 0 & 0 & 0 & 0 \\ 0 & 0 & 1 & 0 & 0 & 0 & 0 & 0 & 0 \\ 0 & 0 & 0 & 1 & 0 & 0 & 0 & 0 & 0 \\ 0 & 0 & 0 & 0 & 1 & 0 & 0 & 0 & 0 \\ 0 & 0 & 0 & 0 & 0 & 1 & 0 & 0 & 0 \end{pmatrix}, D_{\text{CA}} = \begin{pmatrix} 3 & 0 & 0 & -3 & 0 & 0 & 1 & 0 & 0 \\ 0 & 3 & 0 & 0 & -3 & 0 & 0 & 1 & 0 \\ 0 & 0 & 3 & 0 & 0 & -3 & 0 & 0 & 1 \\ 1 & 0 & 0 & 0 & 0 & 0 & 0 & 0 & 0 \\ 0 & 1 & 0 & 0 & 0 & 0 & 0 & 0 & 0 \\ 0 & 0 & 1 & 0 & 0 & 0 & 0 & 0 & 0 \\ 0 & 0 & 0 & 1 & 0 & 0 & 0 & 0 & 0 \\ 0 & 0 & 0 & 0 & 1 & 0 & 0 & 0 & 0 \\ 0 & 0 & 0 & 0 & 0 & 1 & 0 & 0 & 0 \end{pmatrix}, D_{\text{BM}} = \begin{pmatrix} 1 & 0 & 0 & 0 & 0 & 0 & 0 & 0 & 0 \\ 0 & 1 & 0 & 0 & 0 & 0 & 0 & 0 & 0 \\ 0 & 0 & 1 & 0 & 0 & 0 & 0 & 0 & 0 \\ 1 & 0 & 0 & 0 & 0 & 0 & 0 & 0 & 0 \\ 0 & 1 & 0 & 0 & 0 & 0 & 0 & 0 & 0 \\ 0 & 0 & 1 & 0 & 0 & 0 & 0 & 0 & 0 \\ 0 & 0 & 0 & 1 & 0 & 0 & 0 & 0 & 0 \\ 0 & 0 & 0 & 0 & 1 & 0 & 0 & 0 & 0 \\ 0 & 0 & 0 & 0 & 0 & 1 & 0 & 0 & 0 \end{pmatrix}$$

Process and measurement noise covariances $Q_i$ and $R$ are chosen with the following values in all our experiments: $Q_{\text{CV}} = I_9$, $Q_{\text{CA}} = I_9$, $Q_{\text{BM}} = \text{diag}_9(1000)$, $R = \text{diag}_3(400)$.

### 4.2 Dataset

Given the limited amount of real data from confocal microscopy, our proposed systems and baseline are evaluated using 3D synthetic images. The images are generated using a simulator where cells are represented by spheres. For a realistic result, the image is first convolved with a point spread function (PSF) and then Poisson noise is applied by generating each output pixel from a Poisson distribution with a mean value equal to the input pixel intensity. Using such a simulator allows isolating the tracking from the segmentation process in order to better evaluate each part separately, as well as to evaluate the tracking robustness against different levels of signal to noise ratio. The segmentation is a simple thresholding of value $t = 0.5$. An example of the generated sequences is depicted in Figure 2.

Given the importance of evaluating our tracking algorithms against realistic cell migration behaviours, the trajectories of moving HeLA cells are imported from real sequences [de Solórzano et al., 2015] into our generator.

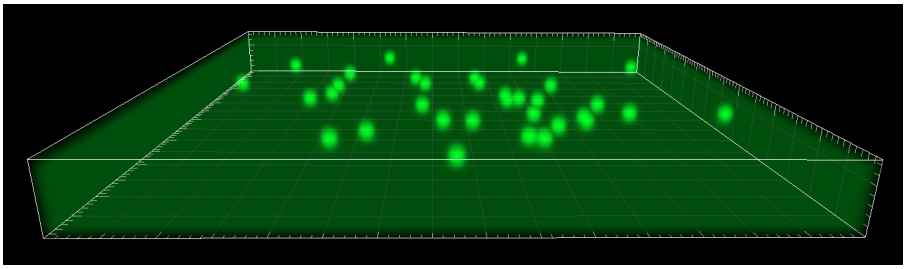

Figure 2: 3D synthetic image of 33 cells, rendered in Imaris

Twelve sequences of increasing complexities, with the number of targets increasing from 8 to 50, are used for testing. Imported trajectories are used as ground truth to calculate the system's performance. Recall and precision, respectively defined in 17 and 18, are used as metrics. A true positive $TP$ is defined for a minimum overlap $b = 0.5$ between estimation and ground truth. A false negative $FN$ occurs when the overlap between estimation and ground truth is inferior to $b$, and a false positive $FP$ is when there is an estimation but no corresponding ground truth.

$$\text{recall} = \frac{TP}{TP + FN} \tag{17}$$

$$\text{precision} = \frac{TP}{TP + FP} \tag{18}$$

### 4.3 Experiments

We compute the recall and precision of all proposed filters for different densities (Table 1), and different noise levels (Table 2). The packing density $\eta$ is the ratio of the total volume occupied by the cells to the total volume considered. For instance, a packing density of $8.0 \times 10^{-4}$ corresponds here to 8 cells in the volume shown in Figure 2.

| | IMM | | Modified IMM | | SIMM | | Modified SIMM | |
|---|---|---|---|---|---|---|---|---|
| Packing density $\eta$ | Recall | Precision | Recall | Precision | Recall | Precision | Recall | Precision |
| $8.0 \times 10^{-4}$ | 0.85 | 0.99 | 0.91 | 1.00 | 0.68 | 1.00 | 0.95 | 1.00 |
| $1.5 \times 10^{-3}$ | 0.79 | 0.99 | 0.85 | 0.99 | 0.66 | 0.99 | 0.88 | 0.99 |
| $2.5 \times 10^{-3}$ | 0.79 | 0.98 | 0.85 | 0.98 | 0.68 | 0.98 | 0.89 | 0.98 |
| $5.0 \times 10^{-3}$ | 0.62 | 0.94 | 0.70 | 0.95 | 0.55 | 0.95 | 0.75 | 0.94 |

Table 1: Results of the experiment without noise

| | IMM | | Mod IMM | | SIMM | | Mod SIMM | |
|---|---|---|---|---|---|---|---|---|
| Max. value of noise distribution | Recall | Precision | Recall | Precision | Recall | Precision | Recall | Precision |
| 50 | 0.78 | 0.53 | 0.84 | 0.51 | 0.63 | 0.55 | 0.91 | 0.46 |
| 30 | 0.54 | 0.61 | 0.58 | 0.57 | 0.51 | 0.63 | 0.65 | 0.49 |
| 10 | 0.03 | 1.00 | 0.03 | 1.00 | 0.03 | 1.00 | 0.03 | 1.00 |

Table 2: Results of the experiment for different noise levels, with $\eta = 8.0 \times 10^{-4}$

### 4.4 Analysis

Table 1 shows that the modification we introduced improves both the performance of the IMM and the SIMM, with a significant increase in the recall, for every packing density value. The precision is always close to 1 because the only source of false positives or distractors in our generator is due to fragmented detections, which are unlikely to happen in data without noise.

Compared to the IMM, the initial version of the SIMM fails to show the results that could be expected according to [Lan et al., 2013]. While this may suggest that second order combination is not suitable for the behaviour displayed by HeLa cells, which is very different from the behaviour of a manoeuvring target, it improves the results when combined with our proposed modification.

The algorithm that yields the best recall is the modified version of the SIMM. Our modification allows the filter to update the model probabilities quicker and take advantage of the second order chain to generate a more accurate estimated state while filtering the mistakes towards the next step predictions. The two SIMM type algorithms are also the ones that resist best when the noise increases, as we can see on Table 2, although none of the methods give acceptable results when the noise level is the highest.

# 5 Conclusion

In this paper, we have described a novel algorithm for multiple cell tracking, which uses an SIMM method, for the first time in biology, in combination with a modified dynamic model prediction. The data association is performed using the greedy linear assignment type. The performance of the algorithm has been tested and compared to a baseline and incremental improved versions, using synthetic data sequences generated from real cells under different density and noise level conditions. Our results show an improvement in terms of recall and precision, compared to the classic IMM and SIMM algorithms.

# Acknowledgments

This work has received funding from the European Union's Horizon 2020 research and innovation programme under the Marie Sklodowska-Curie grant agreement No 642866.

# References

[de Solórzano et al., 2015] de Solórzano, C. O., Kozubek, M., Meijering, E., and Barrutia, A. M. (2015). ISBI cell tracking challenge. `http://www.codesolorzano.com/celltrackingchallenge`. Accessed: 26/05/2016.

[Doucet and Johansen, 2011] Doucet, A. and Johansen, A. M. (2011). *A tutorial on particle filtering and smoothing: fifteen years later*, chapter 24, pages 656–704. Oxford Handbook of Nonlinear Filtering. Oxford University Press.

[Genovesio et al., 2006] Genovesio, A., Liedl, T., Emiliani, V., Parak, W. J., Coppey-Moisan, M., and Olivo-Marin, J.-C. (2006). Multiple particle tracking in 3-d+t microscopy: Method and application to the tracking of endocytosed quantum dots. *IEEE Transactions on Image Processing*, 15(5):1062–1070.

[Gurtner et al., 2008] Gurtner, G. C., Werner, S., Barrandon, Y., and Longaker, M. T. (2008). Wound repair and regeneration. *Nature*, 453(7193):314–321.

[Huang et al., 2009] Huang, B., Bates, M., and Zhuang, X. (2009). Super resolution fluorescence microscopy. *Annual Review of Biochemistry*, 78:993–1016.

[Jaqaman et al., 2008] Jaqaman, K., Loerke, D., Mettlen, M., Kuwata, H., Grinstein, S., Schmid, S. L., and Danuser, G. (2008). Robust single particle tracking in live cell time-lapse sequences. *Nature methods*, 5(8):695–702.

[Kalman, 1960] Kalman, R. E. (1960). A new approach to linear filtering and prediction problems. *Journal of Basic Engineering*, 82(1):35–45.

[Lan et al., 2013] Lan, J., Li, X. R., Jilkov, V. P., and Mu, C. (2013). Second-order markov chain based multiple-model algorithm for maneuvering target tracking. *Aerospace and Electronic Systems, IEEE Transactions on*, 49(1):3–19.

[Meijering et al., 2006] Meijering, E., Smal, I., and Danuser, G. (2006). Tracking in molecular bioimaging. *IEEE Signal Processing Magazine*, 23:46–53.

[Peng, 2008] Peng, H. (2008). Bioimage informatics: a new area of engineering biology. *Bioinformatics*, 24(17):1827–1836.

[Pivarcsi et al., 2004] Pivarcsi, A., Kemény, L., and Dobozy, A. (2004). Innate immune functions of the keratinocytes. *Acta Microbiologica et Immunologica Hungarica*, 51(3):303–310.

[Wilson et al., 2016] Wilson, R. S., Yang, L., Dun, A., Smyth, A. M., Duncan, R. R., Rickman, C., and Lu, W. (2016). Automated single particle detection and tracking for large microscopy datasets. *Royal Society Open Science*, 3(5).